Nanoparticle Assembly

DOI: 10.1002/anie.201006231

Silica-Nanoparticle Coatings by Adsorption from Lysine–Silica-Nanoparticle Sols on Inorganic and Biological Surfaces**

Nicole Atchison, Wei Fan, Damien D. Brewer, Manickam A. Arunagirinathan, Bernhard J. Hering, Satish Kumar, Klearchos K. Papas, Efrosini Kokkoli, and Michael Tsapatsis**

Silica nanoparticles have been used in applications including membranes,[1] catalyst supports,[2] optical devices,[3] chemical/biological sensors,[4] and as building blocks of colloidal and nanoparticle crystals.[5] Furthermore, their relatively low cytotoxicity[6] enables multiple biological applications including dye-doped nanoparticles for cell imaging,[7] drug and DNA delivery,[8] cell surface modification,[9] cell membrane isolation,[10] and sol–gel cell encapsulation.[11–14] Silica nanoparticles are synthesized predominantly using the Stöber method,[15] resulting in narrow distributions of large particles (>200 nm) but broad distributions of smaller particles. Recently, we[16–18] and others[19,20] introduced a method for synthesizing small, monodispersed silica nanoparticles in an aqueous environment in the presence of lysine or other basic amino acids. The approach allows for fine-tuning particle size resulting in silica-nanoparticle sols (hereafter referred to as lys–sil sols) that are stable for months, and also resist aggregation after being dispersed in other solvents including certain cell culture media.[14] It has also been demonstrated that lys–sil sols can form colloidal crystal arrays[20] and thin films by convective assembly.[17] In combination with their tuneable particle size, this translates to capability for precise pore size control.

[*] Dr. W. Fan,[+] D. D. Brewer, Dr. M. A. Arunagirinathan, Prof. S. Kumar, Prof. E. Kokkoli, Prof. M. Tsapatsis
Department of Chemical Engineering & Materials Science
University of Minnesota, Minneapolis, MN 55455 (USA)
Fax: (+1) 612-626-7246
E-mail: kokkoli@umn.edu
tsapatsis@umn.edu
N. Atchison[+]
Department of Biomedical Engineering
University of Minnesota, Minneapolis, MN 55455 (USA)
Prof. B. J. Hering, Prof. K. K. Papas
Schulze Diabetes Institute, Department of Surgery
University of Minnesota, Minneapolis, MN 55455 (USA)
[+] These authors contributed equally to this work.

[**] Funding was provided by the Center for Nanostructured Applications, the Amundson Chair Fund at University of Minnesota, and the NSF (CBET 0956601). Parts of this work were carried out in the Institute of Technology Characterization Facility, University of Minnesota, which receives support from NSF through the NNIN program. Computational support from the Minnesota Supercomputing Institute (MSI) is gratefully acknowledged.

Supporting information for this article is available on the WWW under http://dx.doi.org/10.1002/anie.201006231.

However, convective methods, including evaporation-induced self-assembly (EISA), do not allow manipulation of deposit microstructure since they strongly favor close packing. Moreover, they are not compatible with applications where the substrate cannot be dried, such as living cell encapsulation. In this respect, it is desirable to develop functionalization techniques[21] that enable deposition by adsorption. Here, we report new lys–sil sol syntheses that allow for adjustment of particle charge by surface functionalization. We also report on the inclusion of a fluorescent dye in the silica nanoparticles to be rendered observable by optical microscopy. We then demonstrate tuneable and predictable deposition behavior on inorganic surfaces, as well as layer-by-layer (LBL) assembly for living cell encapsulation. The findings reported here further establish lys–sil sols as a simple and flexible tool for precise colloidal assembly.

To create stable, positively charged silica particles, surface modification was performed with *N*-trimethoxysilylpropyl-*N*,*N*,*N*-trimethylammonium chloride (TMAPS)[22] as well as other functionalizing agents. The modification was assessed with zeta potential measurements as a function of the lys–sil sol pH (Supporting Information, Figure S1). The unmodified silica nanoparticles show slightly negative surface potential at low pH, and the zeta potential decreases to −90 mV when the pH is close to 9.0. The surface potential after surface modification by TMAPS becomes positive when the pH is 7.0 and further increases to around +40 mV when the pH is below 5. Alternative functionalizations and reaction conditions result in distinct behaviors (Figure S1) demonstrating that the surface potential of lys–sil sols can be finely tuned. The modified particles show similar monodispersity, colloidal stability, and evaporative assembly characteristics as those in the original lys–sil sols. By solvent evaporation, three-dimensional colloidal crystals with well-defined mesoporosity can be formed from the surface-modified silica nanoparticles (Figure S2). For optical observation, the silica nanoparticles were labeled with a fluorescent dye. Rhodamine 6G was incorporated by physical adsorption and subsequent capping with a silica outer shell.[23] The UV/Vis absorption spectra for the lys–sil sols with surface-modified fluorescent nanoparticles show maximum absorption at approximately 526 nm, the same as the free dye, and intensity corresponding to five dye molecules per nanoparticle (Figure S3). Photographs of the sols before and after high-speed centrifugation confirm that the dye is present in the nanoparticles (Figure S3 insets). The ability to precisely control fluorescent and nonfluorescent

silica nanoparticle size and surface charge in an aqueous environment free of any stabilizing agent is unique to lys–sil sols and enables precise assembly through colloidal interactions which is described below.

Adsorption of positively charged silica nanoparticles (with radius $a = 10$ nm) on negatively charged glass slides (Gold Seal precleaned micro slides) was performed by immersion (at 4 °C for 30 min) in positively charged lys–sil sols with a constant particle concentration of 0.013 wt % but different ionic strengths. The positively charged lys–sil sols are stable for at least 2 h for all the ionic strengths as confirmed by light-scattering experiments. The coated glass slides were observed with scanning electron microscopy (SEM). SEM images containing approximately 1500 adsorbed particles were processed to determine the final coverage and pair distance distribution function (PDDF). A representative image of the coating made using a positively charged lys–sil sol with $\kappa a = 0.74$, where a is the nanoparticle radius, and κ is the reciprocal Debye length calculated from the ionic strength of the sol, is presented in Figure 1 a. PDDF plots from the deposits formed with increasing ionic strength ($\kappa a = 0.74$, 1.05, 1.48) are shown in Figure 1 b. They exhibit primary peaks (noted by arrows in Figure 1 b), corresponding to the closest distance between adjacent particles. In agreement with the DLVO theory,[24] the average interparticle distance (position of the primary peak) decreases with increasing ionic strength (as shown in Figure 1 b,d and Figure S4). The increase in coverage with ionic strength can be explained in terms of the classical DLVO theory by attributing it to Debye screening of the electrostatic repulsion among the charged particles at the glass surface. At low ionic strengths, when screening is minimal, long-range repulsions limit adsorption due to an excluded-area effect caused by the double layer of ions surrounding an adsorbed particle. At higher ionic strengths, interparticle repulsions are weakened by the screening and the particles form a more dense arrangement.

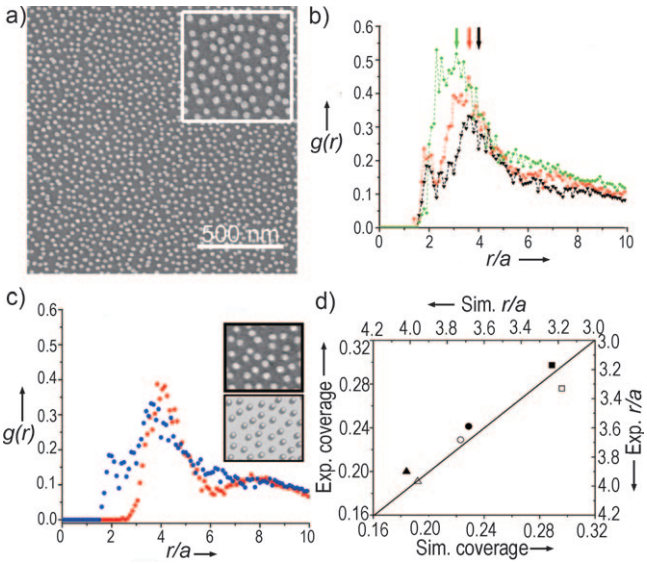

Figure 1. a) SEM image of negatively charged glass slides coated with positively charged lys–sil sols with $\kappa a = 0.74$. b) PDDFs calculated from samples coated under different ionic strengths. Black triangles: $\kappa a = 0.74$, red squares: $\kappa a = 1.05$, green diamonds: $\kappa a = 1.48$. Arrows denote peak positions of the closest distance between adjacent particles. κ^{-1} is the Debye length, r is the interparticle distance and a is the radius of nanoparticles (here $a = 10$ nm). c) Comparison between experimentally obtained PDDF (blue circles) and a Brownian dynamics simulation prediction (red circles) for $\kappa a = 0.74$. For (b) and (c) $g(r)$ is the pair distance distribution and r/a is the radial distance. d) Parity plot of simulated and experimental coverage and interparticle distance for different κa values. The open symbols correspond to coverage, the closed symbols to interparticle distance (r/a). Squares: $\kappa a = 1.48$, circles: $\kappa a = 1.05$, triangles: $\kappa a = 0.74$.

The behavior described above can be quantitatively captured by considering Brownian motion and DLVO (electrostatic and Van der Waals) interactions. The Brownian Dynamics (BD) method based on the Ermak–McCammon algorithm[25] was used to perform simulations corresponding to the experimental conditions (for more details on simulation parameters and methodology, see Supporting Information). The deposit structure and the corresponding PDDF from a simulation with $\kappa a = 0.74$ is shown in Figure 1 c, and compared with the experimentally determined PDDF. SEM images of the adsorbed silica particles and the corresponding configurations observed in BD simulations qualitatively agree. When quantified as PDDF, the experiment and simulation results also qualitatively agree. Some discrepancies may be attributed to particle motion during drying caused by lateral capillary forces. A parity plot of experimental and simulation-derived coverage and PDDF peak positions shows a good agreement between them (Figure 1 d). The random-sequential adsorption (RSA) methodology[26] was also used to simulate the adsorption process. However, a significant discrepancy was observed between the experimental and RSA simulation results (Figure S4), suggesting that surface diffusion and Brownian motion of particles, which are not accounted for in the RSA model, contribute significantly to deposit microstructure development. The results described above demonstrate that the modified lys–sil sols can be used to form predictable nanoparticle arrangements on hard surfaces that can be rationalized by BD simulations incorporating electrostatic and Van der Waals interaction potentials.

Selected experiments further demonstrate the versatility of lys–sil sols for colloidal assembly. For example, we demonstrated that the pH of the sols significantly affects the adsorption results. Almost full coverage was achieved when the adsorption was performed at pH 1.0 (Figure 2 a) where the repulsions between nanoparticles are minimized while there is (apparently) still attraction of nanoparticles to the surface. Moreover, assembly of silica-nanoparticle pairs on the glass surface was achieved by adsorption of negatively charged lys–sil sols on the glass slides that had been coated by positively charged lys–sil sols (Figure 2 b). Finally, controllable particle–particle assembly in solution was demonstrated by using oppositely charged lys–sil sols with different particle sizes. Cryo-TEM (Figure 2 c,d and Figure S5) observation showed that the larger particles were coated by a layer of the oppositely charged smaller ones.

In addition to coatings on hard surfaces and self-assembly in solution, silica nanoparticles are also of interest for biological applications. More specifically, we are interested in creating silica membranes for cell encapsulation. It has

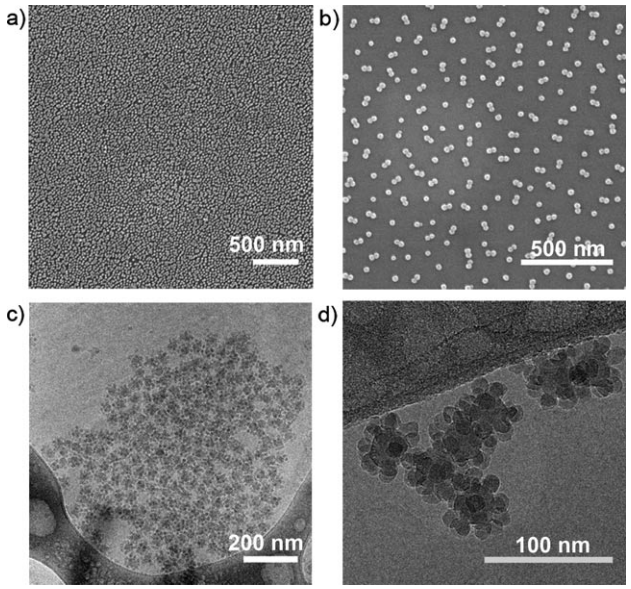

Figure 2. a) SEM image of negatively charged glass slides coated with positively charged lys–sil sols at pH 1.0. b) SEM image of the pair assembly on a glass slide by sequential coating with positively (PEI functionalized) charged and negatively charged lys–sil sols of similar particle size. c,d) Cryo-TEM images of clusters formed by mixing 35 nm positively charged and 12 nm negatively charged lys–sil sols.

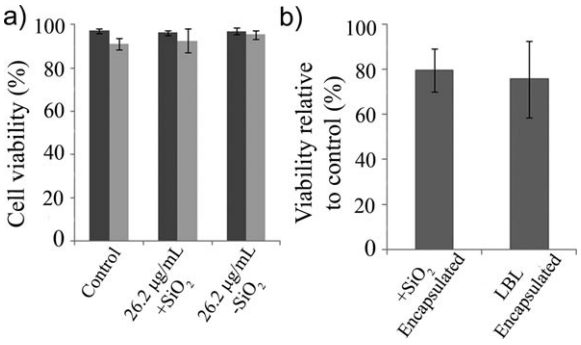

Figure 3. Cytotoxicity of lys–sil sols towards INS-1. a) Trypan blue assessment of cell viability after exposure to 26.2 $\mu g\,mL^{-1}$ of positive or negative lys–sil sols for 30 min in dextrose at 4 °C (dark bars, $n=5$) or 37 °C (light bars, $n=2$). b) MTT assay of INS-1 cells coated with a single layer from 26.2 $\mu g\,mL^{-1}$ positive lys–sil sol or LBL encapsulated with six alternating layers from 26.2 $\mu g\,mL^{-1}$ positive and negative lys–sil sols ($n=3$).

been recognized that the encapsulation of living cells with permselective membranes could substantially prolong the survival of transplanted cells through immunoisolation.[9,27] The ideal permselective membrane would simultaneously protect the cell from immunological attack, efficiently transport nutrients, and rapidly release therapeutic cell metabolites (e.g., insulin). The lys–sil sols are appropriate materials for encapsulation due to the fine pore size control imparted by ability to synthesize very small, monodispersed particles[16,17] with controllable surface charge.

In contrast to previous strategies that use EISA[11] or other deposition processes involving extensive silica polymerization,[12] we aim to form such coatings using layer-by-layer (LBL) assembly. In order to demonstrate deposition of these nanoparticles on living cell membranes, a rat insulinoma β-cell line, INS-1, was used as a model system.[28] Cell membranes are primarily negative and therefore, for the first adsorption positively charged lys–sil sols were used. As the surface charge of modified silica nanoparticles is positive when the pH is below 7, dextrose solution (pH 4.8) was used as a coating solution in all experiments. The stability of silica nanoparticles in dextrose solution is demonstrated in the Supporting Information (Figure S6). The number of silica nanoparticles necessary to form a monolayer around each cell in the sample was determined, and silica was added in concentrations 10-fold (26.2 $\mu g\,mL^{-1}$) this monolayer concentration. Cytotoxicity of the nanoparticles towards INS-1 cells was assessed by trypan blue and MTT assays (Figure 3a and b, respectively). It was found that exposure of INS-1 cells to lys–sil sols at 4 °C or 37 °C was not toxic (Figure 3a). Additionally, encapsulating the cells by a single lys–sil sol layer or LBL assembly (six alternating layers of positively and negatively charged fluorophore-containing lys–sil sols) did not affect cell viability (Figure 3b). Performing LBL assembly in dextrose at 4 °C resulted in good retention of the nanoparticles on the surface of the cell (Figure 4a). Moreover, the addition of 150 mM of the disaccharide trehalose (a cell membrane stabilizer)[29] into the dextrose enabled the INS-1 cells to be coated by LBL assembly at 37 °C (Figure 4b). However, when the coating was attempted at 37 °C in the absence of trehalose the nanoparticles penetrated into the cell (Figure S7). Figure 4c and d show that after 2 and 24 h of culture, respectively, the lys–sil coating is still intact on the cell surface. Figure 4e and f are SEM images of control INS-1 cells at 4 °C and INS-1 cells coated with LBL assembly (six layers) at 4 °C, respectively. Despite the dynamics and complexity of the cell surface, densely packed coatings formed. Next we investigated lys–sil coatings on islets of Langerhans, large clusters of cells, including the insulin secreting β cells. Encapsulation of islets has been studied extensively (for a review, see Ref. [30]) as a means of improving islet survival after in vivo transplantation. Figure 5a and b show porcine islets coated at 4 °C with a single layer of positively charged lys–sil sol and LBL assembly (six layers), respectively. Similar coatings can be obtained at 37 °C in the presence of trehalose. Figure 5c shows that the insulin release response to a tenfold increase in glucose concentration was not significantly different between uncoated islets and islets encapsulated using a lys–sil sol, indicating no adverse effect of the coating on islet function. The simple formation, stability, and demonstrated permeability of the lys–sil sol coatings indicate promise for immunoisolation applications.

In conclusion, size-tuneable fluorescent and nonfluorescent silica nanoparticles with finely controllable surface charge were synthesized in benign conditions. By adjusting the electrostatic interactions, the positively charged silica nanoparticles can be self-assembled onto a smooth surface with opposite charges in a controllable fashion. The coating process and deposit structure can be simulated quantitatively by considering electrostatic and Van der Waals forces and

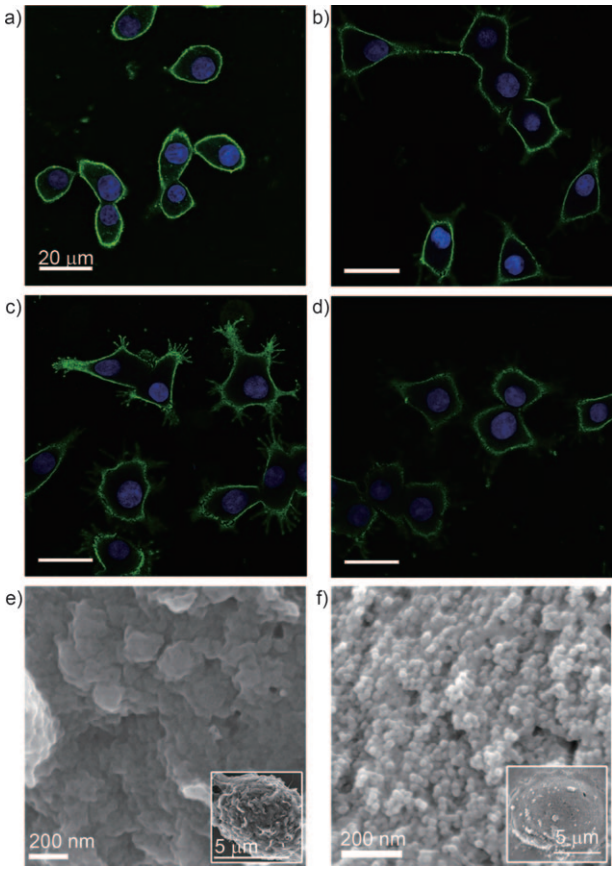

Figure 4. LBL assembly of positively and negatively charged lys–sil sols on INS-1 cells. a) Confocal image of INS-1 cells coated by LBL assembly at 4 °C and b) 37 °C in the presence of trehalose. c) INS-1 cells coated by LBL assembly at 37 °C were cultured for 2 h and d) 24 h at regular culture conditions. Confocal images show cell nucleus (blue) and the lys–sil particles (green). e) SEM images of control INS-1 cells kept at 4 °C and f) INS-1 cells coated at 4 °C by LBL assembly.

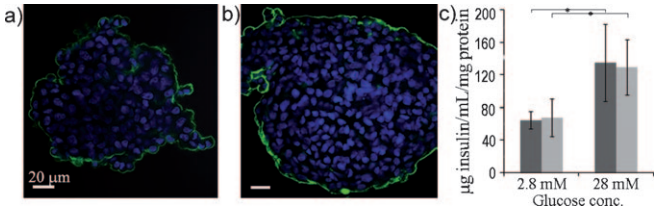

Figure 5. Porcine islets coated at 4 °C with a) positively charged lys–sil sol and b) LBL assembly of six alternating layers from positively and negatively charged lys–sil sols. Confocal images show cell nucleus (blue) and the lys–sil particles (green). c) Glucose-stimulated insulin release data shows islets coated with lys–sil sol (light bars) respond to an increase in glucose concentration in a similar manner to uncoated cells (dark bars). Student *t* test statistical analysis shows a significant difference between the low and high glucose concentrations for both coated and uncoated samples ($n = 5$; *, $p < 0.05$).

Brownian motion. Self-organization of silica nanoparticles by electrostatic interaction at the nanoscale forms a basis for more rational future exploration of colloidal lithography, colloidal membrane formation, and colloidal superlattices. These particles also offer advantages as a membrane material including pore size control, stability, and the ability to be visualized with confocal and electron microscopy. Although here they have been deposited in the absence of polyelectrolytes or other LBL additives, they could also be used in conjunction with such components.[9,31] Their potential applications for living cell imaging and encapsulation were also shown here while the ability to protect the cell from immunological attack and the long-term coating stability are issues under current investigation.

Received: October 5, 2010
Published online: January 7, 2011

Keywords: β cells · encapsulation · islet cells · nanoparticles · silica

[1] A. K. Bohaty, I. Zharov, *Langmuir* **2006**, *22*, 5533; O. Schepelina, I. Zharov, *Langmuir* **2006**, *22*, 10523.
[2] P. M. Arnal, C. Weidenthaler, F. Schüth, *Chem. Mater.* **2006**, *18*, 2733; F. Schüth, A. Wingen, J. Sauer, *Microporous Mesoporous Mater.* **2001**, *44*, 465.
[3] G. A. Ozin, S. M. Yang, *Adv. Funct. Mater.* **2001**, *11*, 95.
[4] Y. N. Xia, B. Gates, Y. D. Yin, Y. Lu, *Adv. Mater.* **2000**, *12*, 693.
[5] H. Hiramatsu, F. E. Osterloh, *Langmuir* **2003**, *19*, 7003; D. Lee, Z. Gemici, M. F. Rubner, R. E. Cohen, *Langmuir* **2007**, *23*, 8833.
[6] J. E. Fuller, G. T. Zugates, L. S. Ferreira, H. S. Ow, N. N. Nguyen, U. B. Wiesner, R. S. Langer, *Biomaterials* **2008**, *29*, 1526; Y. Jin, S. Kannan, M. Wu, J. X. Zhao, *Chem. Res. Toxicol.* **2007**, *20*, 1126; L. Thomassen, A. Aerts, V. Rabolli, D. Lison, L. Gonzalez, M. Kirsch-Volders, D. Napierska, P. Hoet, C. Kirschhock, J. Martens, *Langmuir* **2010**, *26*, 328.
[7] D. R. Larson, H. Ow, H. D. Vishwasrao, A. A. Heikal, U. Wiesner, W. W. Webb, *Chem. Mater.* **2008**, *20*, 2677; W. Law, K. Yong, I. Roy, G. Xu, H. Ding, E. J. Bergey, H. Zeng, P. N. Prasad, *J. Phys. Chem. C* **2008**, *112*, 7972; Y. S. Lin, C. P. Tsai, H. Y. Huang, C. T. Kuo, Y. Hung, D. M. Huang, Y. C. Chen, C. Y. Mou, *Chem. Mater.* **2005**, *17*, 4570; C. Loo, A. Lowery, N. Halas, J. West, R. Drezek, *Nano Lett.* **2005**, *5*, 709; J.-H. Park, L. Gu, G. von Maltzahn, E. Ruoslahti, S. N. Bhatia, M. J. Sailor, *Nat. Mater.* **2009**, *8*, 331; S. Santra, P. Zhang, K. Wang, R. Tapec, W. Tan, *Anal. Chem.* **2001**, *73*, 4988.
[8] D. Luo, E. Han, N. Belcheva, W. M. Saltzman, *J. Controlled Release* **2004**, *95*, 333; F. Torney, B. G. Trewyn, V. S. Y. Lin, K. Wang, *Nat. Nanotechnol.* **2007**, *2*, 295.
[9] H. Ai, M. Fang, S. A. Jones, Y. M. Lvov, *Biomacromolecules* **2002**, *3*, 560.
[10] L. Chaney, B. Jacobson, *J. Biol. Chem.* **1983**, *258*, 10062; V. Gkretsi, Y. Zhang, Y. Tu, K. Chen, D. B. Stolz, Y. Yang, S. C. Watkins, C. Wu, *J. Cell Sci.* **2005**, *118*, 697; D. Stolz, B. Jacobson, *J. Cell Sci.* **1992**, *103*, 39.
[11] H. K. Baca, C. Ashley, E. Carnes, D. Lopez, J. Flemming, D. Dunphy, S. Singh, Z. Chen, N. G. Liu, H. Y. Fan, G. P. Lopez, S. M. Brozik, M. Werner-Washburne, C. J. Brinker, *Science* **2006**, *313*, 337.
[12] G. Carturan, R. Dal Toso, S. Boninsegna, R. Dal Monte, *J. Mater. Chem.* **2004**, *14*, 2087.
[13] E. J. A. Pope, K. Braun, C. M. Peterson, *J. Sol-Gel Sci. Technol.* **1997**, *8*, 635.
[14] M. A. Snyder, D. Demirgöz, E. Kokkoli, M. Tsapatsis, *Microporous Mesoporous Mater.* **2009**, *118*, 387.
[15] W. Stöber, A. Fink, E. Bohn, *J. Colloid Interface Sci.* **1968**, *26*, 62.
[16] T. M. Davis, M. A. Snyder, J. E. Krohn, M. Tsapatsis, *Chem. Mater.* **2006**, *18*, 5814.
[17] M. A. Snyder, J. A. Lee, T. M. Davis, L. E. Scriven, M. Tsapatsis, *Langmuir* **2007**, *23*, 9924.

[18] W. Fan, M. A. Snyder, S. Kumar, P. S. Lee, W. C. Yoo, A. V. McCormick, R. L. Penn, A. Stein, M. Tsapatsis, *Nat. Mater.* **2008**, *7*, 984.
[19] K. D. Hartlen, A. P. T. Athanasopoulos, V. Kitaev, *Langmuir* **2008**, *24*, 1714.
[20] T. Yokoi, Y. Sakamoto, O. Terasaki, Y. Kubota, T. Okubo, T. Tatsumi, *J. Am. Chem. Soc.* **2006**, *128*, 13664.
[21] K. B. Yoon, *Acc. Chem. Res.* **2007**, *40*, 29.
[22] K. N. Pham, D. Fullston, K. Sagoe-Crentsil, *J. Colloid Interface Sci.* **2007**, *315*, 123; A. van Blaaderen, A. Vrij, *J. Colloid Interface Sci.* **1993**, *156*, 1; J. W. Goodwin, R. S. Harbron, P. A. Reynolds, *Colloid Polym. Sci.* **1990**, *268*, 766.
[23] A. van Blaaderen, A. Vrij, *Langmuir* **1992**, *8*, 2921.
[24] J. Lyklema, *Fundamentals of Interface and Colloid Science*, Academic Press, London, **1995**.
[25] D. L. Ermak, J. A. McCammon, *J. Chem. Phys.* **1978**, *69*, 1352; D. D. Brewer, M. Tsapatsis, S. Kumar, *J. Chem. Phys.* **2010**, *133*, 034709.
[26] Z. Adamczyk, M. Zembala, B. Siwek, P. Warszynski, *J. Colloid Interface Sci.* **1990**, *140*, 123.
[27] F. Lim, A. M. Sun, *Science* **1980**, *210*, 908; R. P. Lanza, W. M. Kuhtreiber, D. Ecker, J. E. Staruk, W. L. Chick, *Transplantation* **1995**, *59*, 1377; L. S. Gazda, H. V. Vinerean, M. A. Laramore, C. H. Diehl, R. D. Hall, A. L. Rubin, B. H. Smith, *Cell Transplant.* **2007**, *16*, 609; T. Kobayashi, Y. Aomatsu, H. Iwata, T. Kin, H. Kanehiro, M. Hisanaga, S. Ko, M. Nagao, Y. Nakajima, *Transplantation* **2003**, *75*, 619; Y. Teramura, H. Iwata, *Transplantation* **2009**, *88*, 624; Y. Teramura, H. Iwata, *Biomaterials* **2009**, *30*, 2270; Y. Teramura, Y. Kaneda, H. Iwata, *Biomaterials* **2007**, *28*, 4818.
[28] M. Asfari, D. Janjic, P. Meda, G. D. Li, P. A. Halban, C. B. Wollheim, *Endocrinology* **1992**, *130*, 167.
[29] M. Doxastakis, A. K. Sum, J. J. de Pablo, *J. Phys. Chem. B* **2005**, *109*, 24173.
[30] J. M. Rabanel, X. Banquy, H. Zouaoui, M. Mokhtar, P. Hildgen, *Biotechnol Prog.* **2009**, *25*, 946.
[31] S. Mansouri, J. Fatisson, Z. Miao, Y. Merhi, F. M. Winnik, M. Tabrizian, *Langmuir* **2009**, *25*, 14071.

